Boost Converter with Harvest Regulator Provides High-Efficiency Power Compression for Bio-Hybrid Fuel Cells and Other Weak Energy Sources

David M. Mackie* and Mark R. Morgenstern
U.S. Army Research Laboratory, Adelphi, MD, 20783 USA
*Corresponding Author: david.m.mackie.civ@mail.mil; 301-394-0925

Abstract: Applications for bio-hybrid fuel cells (BHFCs) and other weak energy sources would greatly benefit from highly-efficient power compression that substantially increased the voltage and also allowed intermittent draws of high current. The assumption of a weak energy source necessitates also minimizing parasitic energy draws. We present results for a power compressor composed of a boost converter (variable voltage upconversion), a harvest regulator (matching impedances on the fly), and a bank of low-leakage capacitors (high current draw for short times). The power compressor was not externally powered. Performance was evaluated while connected to two direct ethanol fuel cells (DEFCs) in series, for periods of 3 and 10 days. The DEFCs' design was not optimized for power. They were non-flowing, room-temperature, air-cathode, PtRu/Pt units, which simulated the output of small BHFCs. The power compressor automatically kept the DEFCs close to the voltage yielding maximum power output, which was 400 mV for two DEFCs in series. The output voltage of the capacitor bank was repeatedly raised to 10.25 V and then discharged to 5 V through a resistor. Energy efficiency of the power compressor was uniformly 50%, except for very weak input power.

Keywords: DC-DC converter, fuel cell, boost, harvest, waste-to-energy

1. Introduction

Many novel clean-electric technologies are weak energy sources, in particular biomass/waste-to-energy (B/W2E).[1–5] In traditional B/W2E microbial fuel cells (MFCs), microbes consume "food" (e.g., sugars, acetate, starches, garbage, waste water) and produce excess electrons, which directly drive a fuel cell. Alternatively, microbes can be chosen that produce energy-rich chemicals as metabolic waste (e.g., hydrogen, methane, ethanol). Once refined, these chemicals can be efficiently converted to electricity with a (high-power) chemical fuel cell (FC) – but refining can take 50% of the energy! In bio-hybrid fuel cells (BHFCs), the microbial growth medium is instead refined only by passive filtration, with no energy input to or parasitized from the system, before being passed to an appropriate FC. The biologic, filtration, and FC processes occur continually and simultaneously, as a single interacting system, with minimal external interference. To date, BHFCs have been successfully run with glucose, grape juice, or pulverized apples fermented by yeast into ethanol, which was purified by passive diffusion through a reverse osmosis membrane, and then converted to electrical power with a direct ethanol fuel cell (DEFC).[3]

Published power densities for BHFCs are currently 1–2 mW cm^{-2}. That is two orders of magnitude greater than MFCs.[4,5] Even so, the output voltage of BHFCs is still low for direct use (several hundred mV), so that stacking many cells would be necessary to obtain the threshold voltage levels of standard electronic components and circuits. Due to wide variations in the long-term performance levels of BHFCs (which we will discuss below), connecting many cells together is inadvisable. For good global efficiency, series- or parallel-stacking many cells can be counter-productive, because a worse-performing cell would act as a load on a better-performing cell. Moreover, in many situations where a BHFC would be desirable, the current draw can be sizeable but intermittent, and size/weight/power considerations limit the BHFC area (and thus current). Therefore, a power compressor that raises the voltage and also pulses the current is, in practice, a necessary fourth step in a BHFC, to convert the intrinsic low-voltage and low-current output of the BHFC into a useable form.

In section 2 we describe and explain the three components of the power compressor, concentrating on the harvest regulator's purpose and function. We also give details on the fuel cells used. In section 3 we describe the 3-day and 10-day experiments. In section 4 we discuss the associated results in depth, draw conclusions, and summarize our findings. Appendices A and B contain circuit diagrams and explanations.

2. Experimental Setup

The power compressor used here consisted of a main circuit for voltage up-conversion, which charged a bank of low-leakage capacitors (for current "up-conversion") totaling 56 mF, plus an ancillary circuit to control the main circuit. We stress that this power compressor was *not* externally powered. Since it was dependent upon the very power it was compressing, it had to consume very little power itself. All efficiencies reported here are the full system efficiency, including the parasitic losses to run the power compressor.

DC-to-DC voltage up-conversion was achieved using a boost converter (BC) circuit that we had previously tailored for low-power inputs.[6] The BC topography was chosen due to its simplicity and its ability to switch efficiently at very low frequencies and duty cycle, vastly reducing both component transient and steady-state losses. BCs rely solely on inductive switching to momentarily store energy then transfer power from a low impedance series switch path to a higher impedance barrier diode path. The inductor voltage, therefore, is "boosted" during the transition between the switch on-state and switch blocking. The circuit diagram and parts list for the BC used here are given in Appendix A. Design and simulation details are in reference 6.

While using this BC connected to direct ethanol fuel cells (DEFCs), we noticed an interesting behavior. DEFCs which had become (apparently) exhausted, with too little output power to run the BC, would recover nearly all of their original performance if simply left for a while in an open-circuit condition. (In a subsequent literature search, we found a similar behavior mentioned for direct propanol FCs, where it was attributed to purging the catalytic sites by charge build-up on the anode.[7] Interestingly, a similar behavior has also been noted for microbial fuel cells.[8])

To capitalize on this recovery behavior, an ancillary circuit was added to our tailored BC as a harvest regulator (HR) to handle long-term performance variation in the fuel cells. A CMOS comparator circuit cycled power to the oscillator and gate driver circuits. The HR added only a negligible amount of control power cost. Using circuit simulation results from PSpice and measurements from prototypes (data not shown), we tested the effects of different HR locations. Placing the HR so that it cycled the oscillator and gate drive circuitry on/off also caused the BC's input impedance to cycle between very low/high impedance, respectively. This was functionally equivalent to directly gating the connection between the fuel cell and the BC, but lowered the parasitic effect of the power compressor by two orders of magnitude.

The entire power source used to collect the data displayed in the remaining figures is shown schematically in Figure 1, with one alteration: DEFCs were substituted for BHFCs. Ethanol was added to the DEFCs in percentages comparable to what yeast would supply to the DEFC component of a BHFC. This simplified the system for experimental convenience. Doing so increased repeatability and decreased overall run times (from weeks to days).

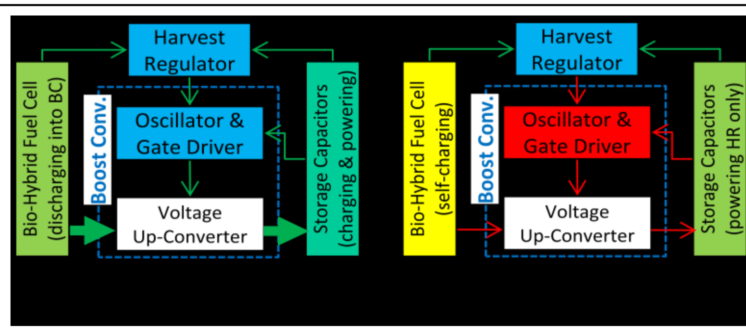

Figure 1. Complete bio-hybrid fuel cell power source including harvest regulator (HR). The control circuitry, which includes the HR, oscillator, and gate driver, requires three orders of magnitude less power than the total (average) pass-through power of the power compressor. Thin/thick lines represent high/low impedance connections, respectively. Components are color-coded as follows: green = providing power; blue = consuming power; aqua = both providing and consuming power; red = shut off. The voltage up-converter is white, to indicate that it is a passive component, converting power between its input and output. Its low/high impedances are determined by the on/off states of the oscillator & gate driver component.

With the HR cycling the BC on and off within a user-defined hysteresis band, the DEFC voltage can effectively be regulated and the overall input impedance of the BC can be matched to that of the DEFC at a particular voltage. For all experiments presented here, the HR hysteresis band was roughly 100 mV. For example, with the HR level set to 400 mV, the HR toggled the system to the "off" state whenever the DEFC voltage fell to 350 mV, and toggled the system to the "on" state whenever the DEFC voltage rose to 450 mV. (All voltages in this paper are DC.)

An entirely separate circuit periodically discharged the capacitor bank. Unlike the BC-HR, this circuit was externally powered, since it was essentially measuring the performance of the power compressor, rather than being part of the power compressor *per se*. (However, external power is not essential, since this is not a power-hungry task. In ref. 5 we powered similar circuitry internally.) When the voltage on the capacitor bank, V_{CAP}, reached 10.25 V, this tracking circuit discharged the storage capacitors through a 200-Ω load until V_{CAP} was 5.00 V. This range for V_{CAP} was chosen based upon the voltage needs of standard electronics. The resistor value was chosen to discharge the capacitors quickly but without any risk of damaging them.

The DEFCs were made using commercial membrane electrode assemblies (MEAs) obtained from FuelCellsEtc. (College Station, TX, USA). The proton exchange membrane (PEM) was Nafion117, with 4 mg cm^{-2} platinum-ruthenium catalyst on the anode side and 4 mg cm^{-2} platinum black catalyst on the cathode side. The electrodes were carbon mesh. The current collectors were 35-mil thick stainless steel with 202 through-holes that were $\frac{1}{16}''$ (62.5 mil) diameter, in a triangular (*i.e.*, face-centered hexagonal) pattern, with centers 77.5 mil apart. The hole design for the current collectors had to balance machinability and various performance factors. The triangular lattice can be broken down into two interwoven rectangular lattices, and is thus easily programmed into a computer-controlled drill. The chosen parameters gave a large fill factor for the holes (60%, desirable to maximize transport to and from catalytic sites), kept the smallest metal width from becoming too small (15 mil, desirable for strength and conductivity, and to prevent pressure-cutting the MEA), and kept the non-metal transport distance small (less than 31.3 mil, desirable for low internal resistance). The DEFCs had air cathodes, with no fans or atmospheric controls. The active area was 6.8 cm^2, and the anode chamber volume was 10.0 mL. The fuel was 11% (v/v) ethanol in deionized water, and was delivered in batch mode (no flow), with a single fill at time zero unless otherwise stated.

All voltages were recorded once per second with a digital oscilloscope (Yokogawa DL750 ScopeCorder).

3. Results

Figure 2 shows a 2600-second sample of the basic waveforms of the converter, during day 3 of a 4-

day run. Both the BC and the load operate intermittently, and over different timescales. The period for each varies with fuel cell performance. This intermittency increases efficiency by matching impedances, and scales up output power to more useable levels.

The fuel cell voltage, V_{FC}, (blue, serration-shaped line) is input to the BC. During the "on" state, the fuel cell provides the BC with a pulse of input power, P_{IN}, (black dots connected by thin black line) from 8 to 5 mW, as V_{FC} falls from the top to the bottom of the HR hysteresis band. The BC's output, stored in the 56 mF bank of storage capacitors, is measured as V_{CAP} (red, staircase-shaped line).

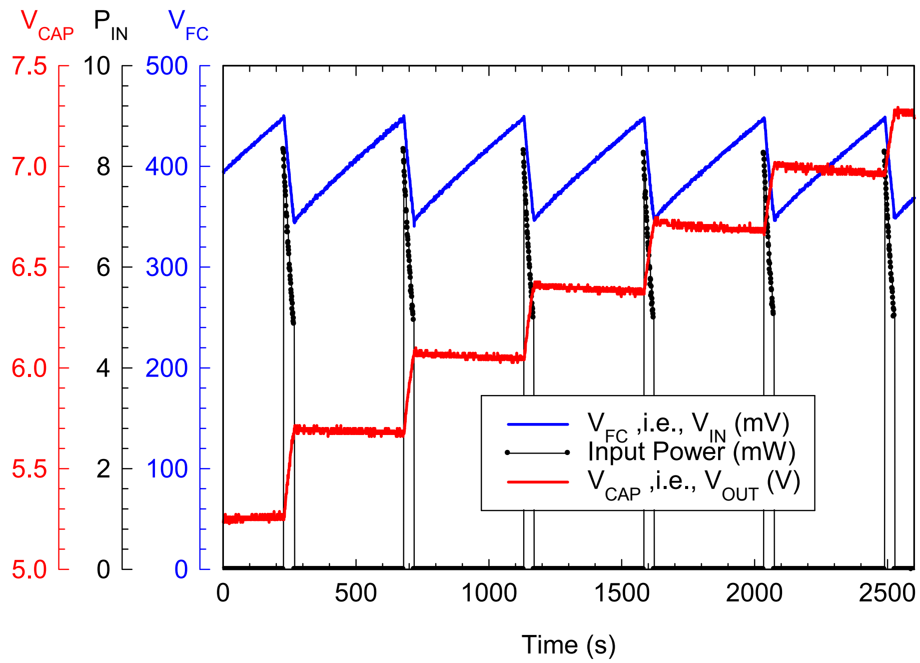

Figure 2. A 2600-second sample of the basic waveforms of the converter, during day 3 of a 4-day run. The fuel cell voltage, $\boldsymbol{V_{FC}}$, (blue, serration-shaped line; rightmost abscissa) is input to the BC. The spikes of input power, $\boldsymbol{P_{IN}}$, during "on" states are shown as black dots connected by a thin line (middle abscissa). The BC's output, $\boldsymbol{V_{CAP}}$, (red, staircase-shaped line; leftmost abscissa) is stored in the capacitor bank. It is stepping up to 10.25 V. In this sample the fuel cell performance has degraded so that stored energy noticeably depletes during "off" states.

V_{CAP} steps up each time V_{FC} steps down, with a magnitude that lessens as V_{CAP} increases (while the V_{FC} step-down remains constant). Eventually V_{CAP} will reach 10.25 V and will discharge down to 5 V through a resistor (not shown in Fig. 2). The output capacitor will still charge when connected to a nominally performing fuel cell (as in Fig. 2), but at a slower and less efficient rate. Also, note that V_{CAP} slowly decreases during the "off" state. This off-state decrease, initially barely noticeable, becomes significant as a run continues for several days. Barring intervention, the fuel cells eventually take so long to go from the bottom to the top of the HR hysteresis band that the off-state degradation during that time is as large as the on-state step-up for higher voltages. At that point, the power source is effectively dead even though the fuel cells continue to operate.

The determination of P_{IN} is described in ref. 5; we summarize here for convenience. The input voltage, V_{IN} (*i.e.*, V_{FC}), is easy to measure, but the input current, I_{IN}, is not. Because the BC impedance is so small, adding even a small series resistance to measure I_{IN} seriously degrades BC performance. Hall Effect sensors had inadequate signal-to-noise. Instead, we used the good approximation

$$P_{IN} \cong \frac{1}{2} D\, I_{peak}\, V_{FC} \tag{1}$$

where the duty cycle, *D*, was 0.2, and where I_{peak} is given by

$$I_{peak} = \frac{V_{FC}}{Z}\left(1 - e^{-\frac{Z\,\tau}{L}}\right) \tag{2}$$

where *Z*, τ, and *L* are the BC's impedance, charging time, and inductance, respectively, and are all known quantities. Putting in those known quantities gives

$$P_{IN} \cong 41.1 \frac{mW}{V^2} {V_{FC}}^2 \tag{3}$$

Since the BC's output power, P_{OUT}, was used to charge a capacitor bank with total capacitance *C*, it was easily determined from the standard equation

$$P_{OUT} = C\, V_{CAP}\, \frac{d}{dt}(V_{CAP}) \tag{4}$$

with the instantaneous time derivative approximated by a simple difference. (Recall that voltage measurements were taken once per second, which was more than adequate for our purposes.)

Several experiments were performed in order to assess the long term performance of the BC-HR combined with DEFCs. In the first set

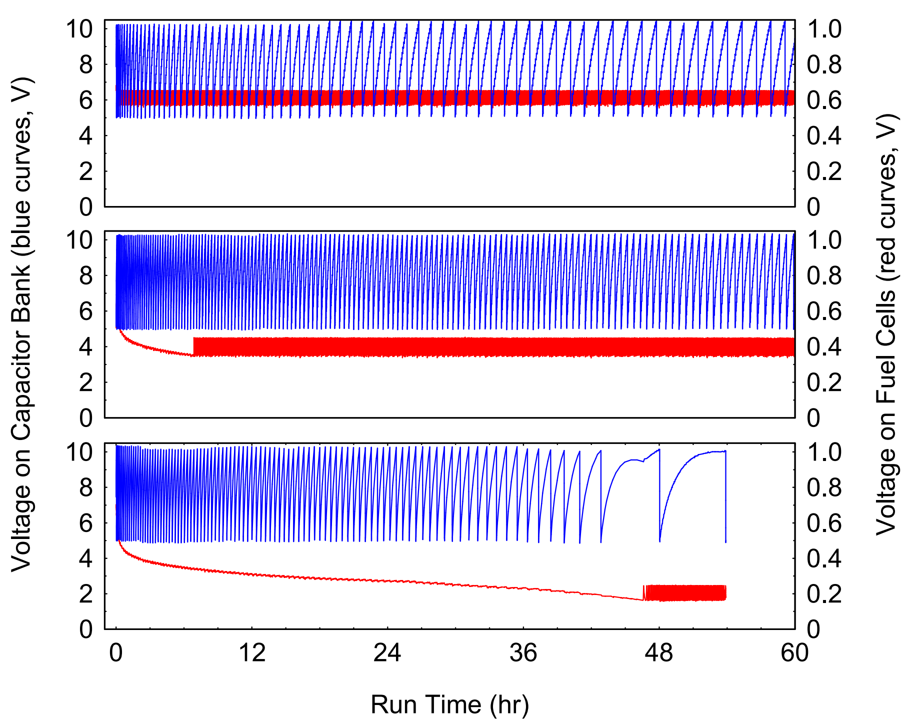

Figure 3. Performance over 60 hr of this paper's BC-HR for three HR settings (top to bottom: 0.6 V, 0.4 V, 0.2 V), showing the voltages on the fuel cells (i.e., the BC-HR input, red lines, right abscissa) and the voltages on the 56 mF capacitor bank (i.e., the BC-HR output, blue lines, left abscissa), when the BC-HR is powered by two DEFCs in series, fueled once at Run Time = 0.

of experiments, two DEFCs (detailed above) were connected in series as a power source. They were fueled once at Run Time = 0, and run for 72 hr (when possible). The HR was set to various levels.

Figure 3 shows the voltages on the fuel cells (i.e., the BC-HR input, red lines, right abscissa) and the voltages on the 56 mF capacitor bank (i.e., the BC-HR output, blue lines, left abscissa) over 60 hr, for three HR settings (top to bottom: 0.6 V, 0.4 V, 0.2 V). For 0.6 V and 0.4 V, the harvest cycling begins fairly quickly (about 2 and 7 hr, respectively). In contrast, for 0.2 V, the harvest cycling doesn't begin until the DEFCs are performing quite poorly. Starting at about 47 hr, the HR is able to rescue the penultimate capacitor bank charge, and add one more. After that, the voltage recovery by the DEFCs is so slow that the BC output power during "on" times can't keep up with the drain on the storage capacitor depletion during the long "off" times.

This failure mechanism is clearly seen in Figures 4 and 5, which analyze the data sets from Figure 3 plus another data set (HR@500mV). Figure 4 shows performance (over 72 hours) for the four HR settings, in terms of time (in minutes) to recharge the capacitor bank. (For the HR@200mV run, the final few recharging times are well beyond the abscissa range.) Figure 5 shows the performance in terms of average output power, P_{avg}, and cumulative output energy, E_{cum}. P_{avg} is the energy per discharge (E_{dis}, 2.24 J) divided by the run time between discharges. E_{cum} is E_{dis} multiplied by the number of discharges.

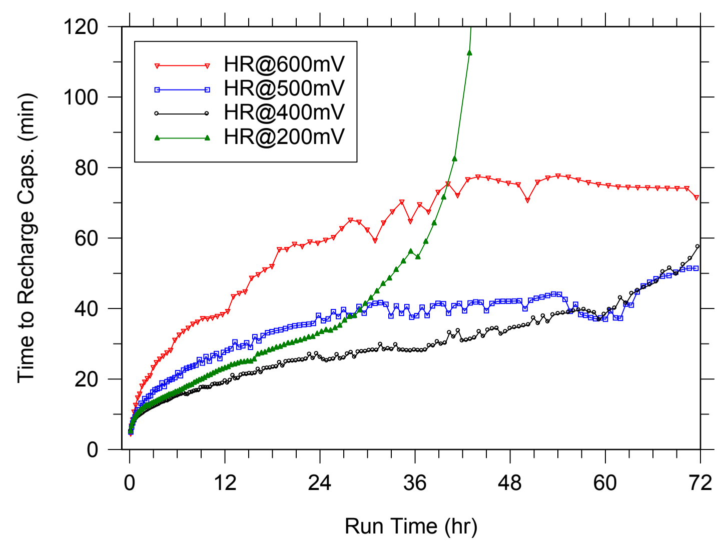

Figure 4. Performance over 72 hr of this paper's BC-HR for four HR settings, in terms of time (in min) to recharge the 56 mF capacitor bank from 5 V to 10.25 V, when the BC-HR is powered by two DEFCs in series, fueled once. For the HR@200mV run, the final few recharging times are well beyond the abscissa range.

Both 400 and 500 mV for the HR level gave good results, with the 400-mV HR level slightly outperforming for the first 50 hours. This was not entirely unexpected, since previous experiments (for short run times of < 1-hr) had shown that the power curve for these DEFCs peaked at 200 to 250 mV (and there were two DEFCs in series). It was surprising, though, that the short-term power curve apparently remained valid over such long runs. After 72 hours, the performance of the 400- and 500-mV HR levels is identical (and not much better than the performance of the 600-mV HR level). This can be seen by the time to recharge (Fig. 4) and by P_{avg} (Fig. 5, lines+markers, left abscissa). However, the performance head-start of the better-performing HR levels won't be easily overcome by running for longer times (say 96 hr), as is clearly seen by E_{cum} (Fig. 5, lines only, right abscissa). By 72 hr, the average power for all cases is quite low (<1mW), so the large differences in E_{cum} will likely not change much, although our data can't rule out the possibility.

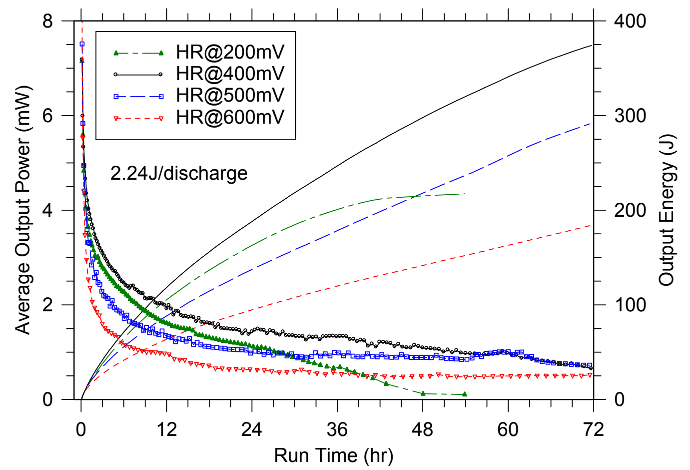

Figure 5. Performance over 72 hr of this paper's BC-HR for four HR settings, in terms of average output power in mW (P_{avg}, lines+markers, left abscissa), and cumulative output energy in J (E_{cum}, lines only, right abscissa), when powered by two DEFCs in series, fueled once. For clarity, the individual data points are left out of the E_{cum} plots.

For the 200-mV HR level, the DEFCs were free-running most of the time. This worked well initially – even better than the 500-mV HR level – but by 24 hr the input voltage to the BC had dropped to 3 mV (compare Fig. 3). For times after that, as the input voltage dropped lower and lower until it averaged 200 mV, it is obvious that the BC's output power was being generated inefficiently. It took longer and longer to recharge the storage capacitor bank. By 46 hours, the input voltage had dropped so low that less energy was coming into the storage capacitors than was being drawn off to run the BC-HR circuitry. When the HR cycling finally took effect, it was able to raise the average input voltage slightly, which gave just enough of an efficiency increase to allow completion of a few more capacitor discharges.

Although we knew *a priori* that the 600-mV HR level would be difficult for the DEFCs to maintain (300 mV each), we also knew that the BC was more efficient at converting higher input voltages. The data show, however, that the decreased DEFC efficiency more than made up for the increased BC efficiency.

In the second experiment, two DEFCs were connected in series to our BC-HR-based power compressor and run for 10 days. See Figure 6, where we show V_{CAP}. The 330 discharges of V_{CAP} produced 740 J of useable energy. Note that the time scale is changed several times in the chart, and is in hours. Based on the results shown in Figs. 3–5, the HR level was set to 400 mV. During this 10-day experiment the fuel was periodically "topped off" to offset evaporation and usage. In this way, a total of

35 mL of fuel was eventually put into the two 10-mL anode compartments. Even while the DEFC performance gradually declined, the power compressor's efficiency remained at roughly 50% the majority of the time.

At several points in the experiment, the DEFCs were allowed to run for long periods (e.g., weekends) with no fuel added. This is seen most clearly prior to 93 and 208 hours. DEFC performance degraded to where their energy could be harvested by the BC-HR only a small percentage of the time. The ethanol concentration had been greatly reduced, and the DEFC reaction product (acetate) had built up. Plus, the liquid had evaporated to about ¾ its original height in the DEFCs, which reduced the DEFCs' working area. At those points the average output power declined to where the power required for the control circuitry (approximately 70 μW) was comparable to the overall converted power, and efficiency of the power compressor declined exponentially. However, once the fuel was topped off again, the performance and efficiency of the power compressor returned almost to its original level.

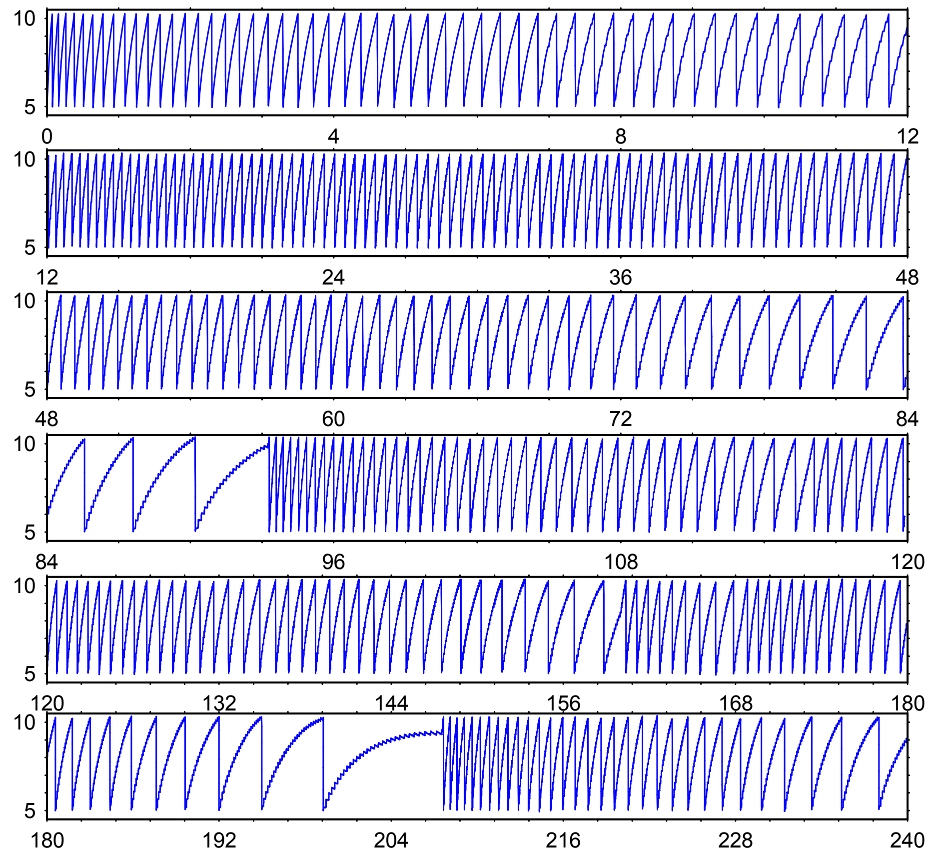

Figure 6. Voltage across a capacitor bank (56 mF), $\boldsymbol{V_{CAP}}$, at the output of the BC, as a function of time, for two DEFCs connected in series as a power source and run for 10 days, fueled several times. The HR was set at 400 mV. The capacitors were repeatedly charged by the BC and then discharged through a 200 Ω load. This occurred 330 times during the 10 day test. The power compressor produced 740 J of *useable* energy. Note that the time scale is changed several times in the chart, and is in hours. Major refuelings took place at 93, 160, and 208 hr.

Figure 7 contains summarized analysis for the second experiment. Each of the five plots is derived from the data in Figure 6, but averaged over 8 hr to suppress short-term fluctuations. It is clear that, with two well matched fuel cells connected in series as a power source, the power compressor performance is very stable. Not surprisingly, the average input voltage (*i.e.*, fuel cell voltage, closed blue circles) stays within 10 mV of the HR setting. The average output voltage (*i.e.*, capacitor bank voltage, closed red squares) remains close to 8 V, except when the DEFCs are performing especially poorly from lack of fuel. At those times (notably near 93 and 108 hr, cf. Fig. 6), the average output voltage increases, while the input power (open blue circles) and output power (open red squares) drop.

The effect of the three major refuelings can be observed as upward jumps in the average input and output powers. However, the power compressor's global efficiency (open black triangles) holds steady at close to 50%, despite the average input power dropping from 190 mW down to 20 mW. Efficiency only varies significantly after extreme changes in fuel cell performance, as is seen in the data point for 200–208 hours.

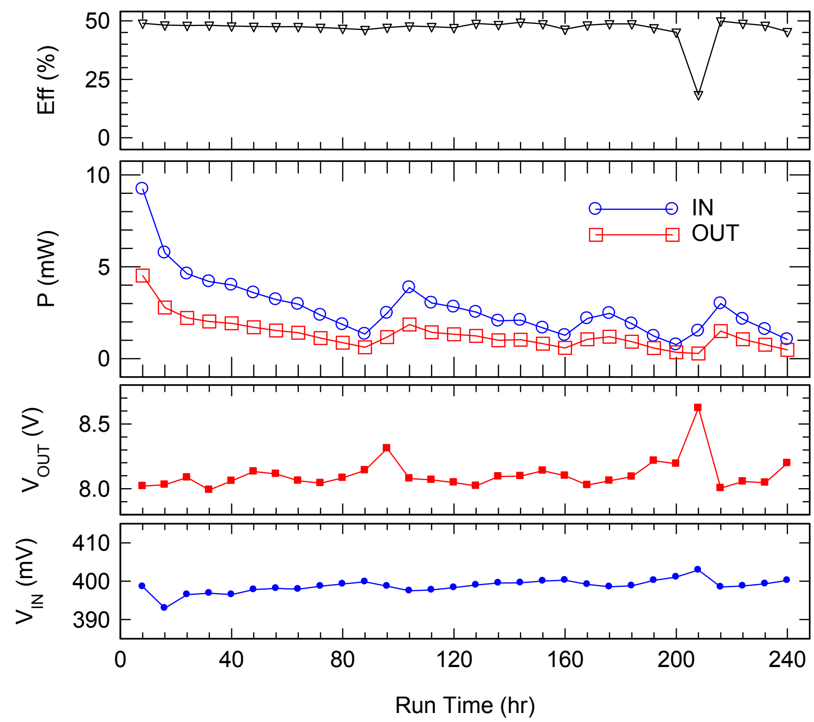

Figure 7. Analysis of Second Experiment (cf. Fig. 6). In the 5 plots of this figure, the data is averaged over 8 hr to suppress short-term fluctuations. With two well matched fuel cells connected in series as a power source the converter performance is very stable.

4. Discussion and Conclusion

During the first 8 hours of the second experiment, the (combined) DEFC voltage never falls below the turn-off threshold of 360 mV and the converter is on 100% of the time. Nevertheless, most of that 8 hours the input voltage is less than 500 mV, which hurt the global efficiency. Early on, when the input voltage was 600 mV, the global efficiency was 60%. These global efficiencies should be compared to the (higher) inherent efficiencies of the BC. In Figure 8 we plot (using data from ref. 5) the BC efficiency as a function of the output voltage (corresponding to V_{CAP}), for different values of the input voltage (corresponding to V_{FC}). For the BC-HR of this study, we could not quite achieve such high efficiencies because the input voltage was not on continuously.

Our design accounted for the discontinuous input voltage to the BC by turning off the BC when it was not needed, but the HR still needed to be powered continually. In Figure 9 we plot the power required by the HR at output voltages (V_{CAP}) ranging from 6–9 V. This power is very low (~1%) compared to the 1–5 mW converter output power levels seen in normal operation. (Compare Fig. 5.) However, when the DEFCs were low on fuel, the BC-HR spent an inordinate percentage of its time in the "off" state, raising the DEFC voltage to the discharge level (*i.e.*, raising it from 350 to 450 mV). The low power to run the HR integrated over that long time works out to a non-negligible expenditure of energy.

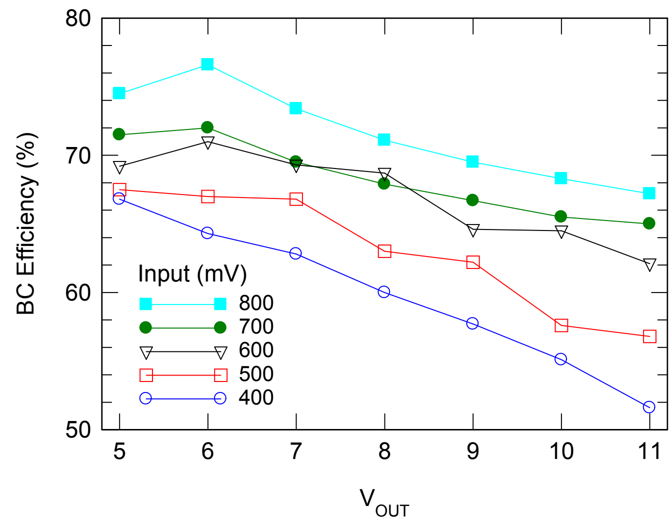

Figure 8. Inherent efficiency of the boost converter (BC), as a function of output voltage, for different values of the input voltage. (After Ref. 6)

Nevertheless, we expected a slightly better global efficiency of about 60% during normal operation. Suspecting that the capacitor bank might be leaking charge in a faulty manner, we looked closely at the voltages, and found an unexpected problem. During discharges of the capacitor bank, we had assumed V_{FC} would remain constant. Instead, V_{FC} was dropping. This was especially evident at early times, while the DEFCs were first "powering up" from their storage/cleaning state. For the first few hours, V_{FC} was actually steadily rising – *except* during discharges of V_{CAP}, when it would fall dramatically. The explanation is rather complicated, and references the circuit diagram in Appendix A.

Recall that when an inductor is dissipating its energy, its current is set by its changing magnetic field. In our

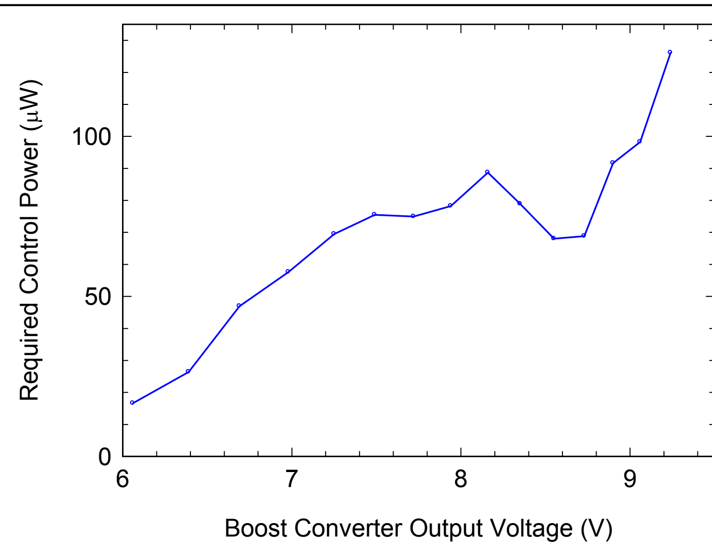

Figure 9. Power required for boost converter control circuitry at voltages ranging from 6–9 V. This power is very low compared to the 1–5 mW converter output power levels seen in normal operation. (Compare Fig. 5.)

device, at the first instant after the MOSFET turns off, the inductor current remain approximately at the same level as it was right before switch turn-off. With the inductor dissipating its magnetically stored energy, it behaves as a true current source and the voltage across it is determined by the impedance across it. The diode-to-capacitor-bank connection then becomes the load of the inductor because it is then the lowest impedance.

In other words, when the MOSFET turns off, the energy that the inductor stored while the MOSFET was on is rerouted through the barrier diode to the output capacitor and load resistor. This is what allows this circuit to boost voltage because the new higher impedance sets the new voltage. The inductor's collapsing magnetic field produces an electric field that seeks to equalize itself through the path of least resistance. (The barrier diode is located between the inductor and the output capacitor. It allows energy to be put into the output capacitor but not come back out when the MOSFET turns back on.)

When the inductor field dissipates to the point that it no longer has the EMF necessary in order to forward-bias the barrier diode, the inductor still has some of its energy left over. With a momentary connection into a very large impedance, according to Lenz's Law, the voltage of the inductor reverses, producing a negative voltage at the drain of the MOSFET.

This forward-biases the MOSFET's body diode, and the remainder of the inductor energy is back-fed into the fuel cell. (As is common, our MOSFET switch has a parasitic anti-parallel diode built into its basic structure.) Normally, this body diode increases the BC's efficiency because it allows the inductor to put back some unused energy after its EMF falls below what is necessary to forward bias the barrier diode. The back-feeding adds charge back into the fuel cell, since a negative voltage is applied to the cathode of the fuel cell.

However, during a capacitor bank discharge, the impedance of the barrier diode is dropping while the inductor is dissipating its field though the barrier diode. This results in a longer-than-usual diode on-time, and so less energy is left in the inductor to back-feed to the fuel cell. This is seen as a drop in VFC, because the fuel cell must supply energy to the inductor that it normally doesn't have to supply.

This means that, during a capacitor bank discharge, extra energy is being consumed from the fuel cell, but in an indirect way. This energy is going to the discharge resistor as useful power, but is not accounted for in our analysis, which measures only the change in VCAP. Thus, our actual global efficiency is higher than reported.

In summary, we presented an energy-efficient power compressor circuit for low-power sources (low voltage combined with low current) such as bio-hybrid fuel cells, that can power conventional electronic circuitry. The power compressor was composed of a combination of harvest regulator (HR), boost converter (BC), and capacitor bank. The HR effectively matched changing fuel cell impedance to constant BC impedance in order to maintain an optimal power transfer between the fuel cell and the BC. The overall average impedance of the BC input was modulated by the HR by power cycling the BC according to the current performance level of the fuel cell. This ensured that the efficiency of the BC remained at close to its maximum for the chosen input and output voltages, without regard to fuel cell performance levels (except for extreme variations). This provided consistency in performance over long periods of operation (3 to 10 days).

In our experiments, the efficiency performance of the converter remained stable except for when the fuel cells ran almost completely out of energy. Average efficiency, input voltage, and output voltage remained relatively constant over a 950% variation in power being harvested from the fuel cell. Thus the HR-BC power compressor was able to convert half of the energy produced by the DEFC to energy *directly useable by common electronic devices*, even when the DEFCs were running low on fuel, and even after 10-day runs when they were contending with accumulations of their waste acetic acid.

Appendix A: Boost converter circuit [ref 6]

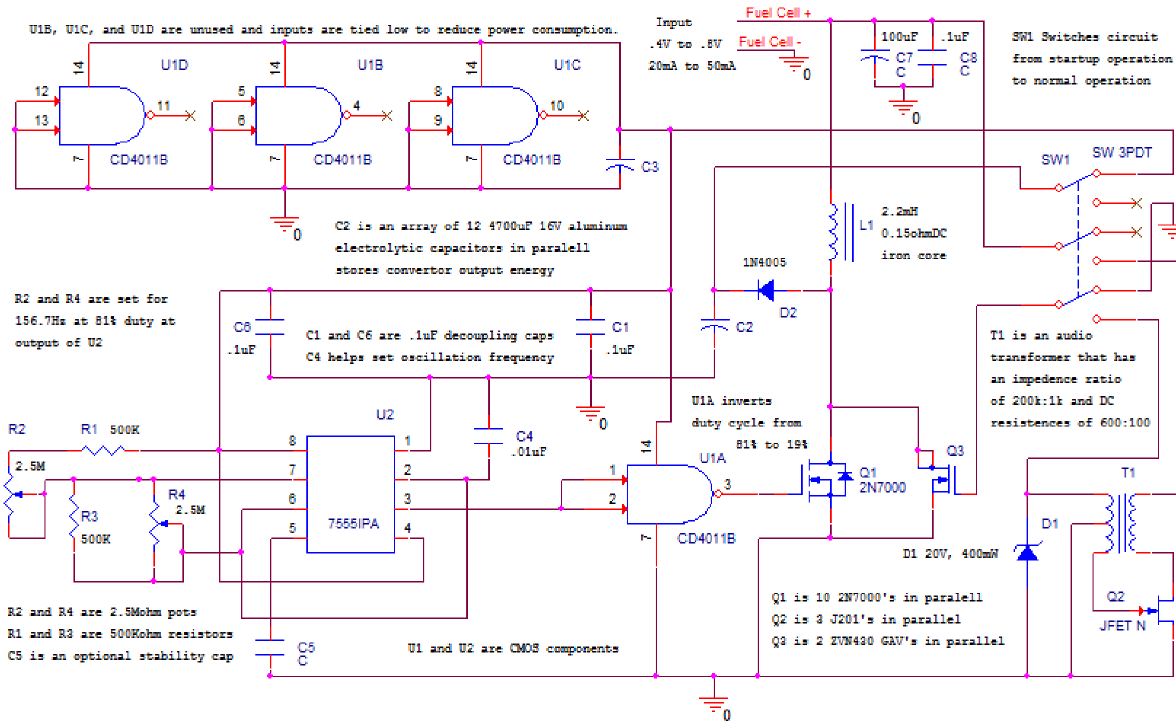

Figure A1. Boost converter circuit previously tailored for low-power inputs [ref 6].

Qty	Part Number/Value	Description
1	CD4011B	CMOS quad NAND-gate
1	7555IPA	CMOS version of 555 timer
2	2.5 MΩ	2.5 MΩ trimmer pot 0.125 W
2	500 KΩ, 0.125 W	carbon resistor
2	0.01 µF	capacitor
5	0.1 µF	tantalum capacitor
10	2N7000	N-channel small signal MOSFET 60 V, 200 mA
2	ZVN 430 GAV	N-channel MOSFET 60 V, 2.1 A
1	1N4005	general purpose silicon diode
3	J201	N-channel JFET
1	–	panel switch 3PDT
1	–	audio transformer 200k:1k impedance ratio, 600:100 DC resistance ratio
1	2.2 mH, 0.15 ΩDC	Janzten audio sub-woofer cross-over inductor
1	100 µF	tantalum capacitor
12	TVX1C472	4700 µF aluminum electrolytic capacitor
1	1N520B-TP	20 V, 40 0mW Zener diode

Table A1. Parts list for boost converter circuit [ref 6].

Appendix B: Harvest Regulator Circuit

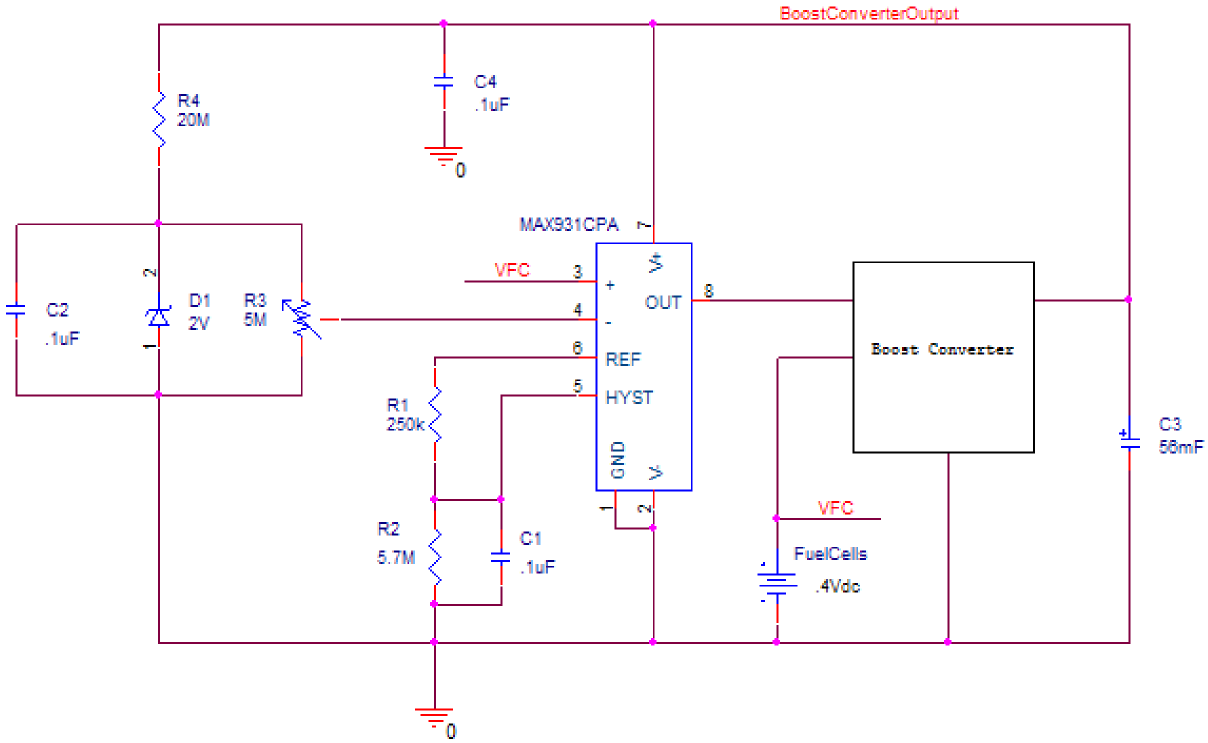

Figure B1. Harvest Regulator Components and Associated Circuitry

The main component of the harvest regulator (HR) is a MAX931CPA CMOS comparator integrated circuit (IC). The output of the MAX931CPA can source 40 mA of current, which is two orders of magnitude more than what is required for the oscillator (OSC) and gate drive (GD) ICs of the boost converter (BC) of Appendix A. Q1 in the schematic in Appendix A is an array of several N-channel MOSFETs and are normally off devices. If power is removed from the OSC and GD ICs of the BC a zero current draw from the fuel cells (FCs) by the BC will result. The output of the MAX931CPA provides a power source for the OSC and GD and therefore gates the entire BC on and off without placing a switch directly in line with the FC output. This provides us with the power cycling benefit of the HR but without most of the DC losses that would otherwise result if the HR directly switched the FC output.

The sub-circuit consisting of R4, C2, D1, and R3 sets the voltage reference by which the FC output is compared. R4 limits the current draw to 500 nA at 10 V. D1 and C2 provide a reliable 2-V reference for R3, despite the wide variation of the BR output. The average voltage level at which the HR keeps the FCs is adjusted with R3.

The sub-circuit comprising of R1, R2, and C1 sets the width of the HR's hysteresis band, VHB. For this experiment V_{HB} was set to 100 mV. C1 provides some noise immunity. R1 and R2 are determined by the following equations:

$R1 = \frac{V_{HB}}{(2I_{REF})}$, and $R2 = \frac{(1.182 - \frac{V_{HB}}{2})}{I_{REF}}$, where $I_{REF} = 200$ nA.

C3 is the storage capacitor bank, comprising twelve aluminum electrolytic capacitors in parallel totaling 56 mF. The BC output power is integrated and stored for intermittent load draws. The HR is always connected to the BC output; however, its current draw is negligible (usually not more than 10 μA).

For experimental convenience an external DC reference was used in place of R3, however R3 was left in the circuit as a path of DC leakage from the BC output to ground. The external DC reference, therefore, only contributed a negligible 5 nA or less to the overall system because 5 nA is the maximum current leakage of pin 4 of the MAX931CPA. The voltage at pin 3 (the fuel cell voltage or V_{FC}) is being compared to the reference provided at pin 4 and must be greater than the reference for pin 8 to go to a logic high. Specifically, if MAX931CPA's pin 4 is set to 400 mV and V_{HB} is set to 100 mV, then the BC will cycle on and off between a FC output of 350 mV and 450 mV.

Expanded References (with Titles) for Reviewers' Convenience

[1] D.M. Mackie, S. Liu, M. Benyamin, R. Ganguli, and J.J. Sumner, Direct Utilization of Fermentation Products in an Alcohol Fuel Cell, *J. Power Sources* 232, 34–41 (15 June 2013).

[2] R.C. Saxena, D.K. Adhikari, and H.B. Goyal, Biomass-based energy fuel through biochemical routes: A review, *Renewable & Sustainable Energy Reviews* 13, 167–178 (2009).

[3] P. Malati, P. Mehrotra, P. Minoofar, D.M. Mackie, J.J. Sumner, and R. Ganguli, Forward Osmosis-Integrated PEM Fuel Cell for Converting Fermenting Biomass to Electricity, submitted to *Energy and Environ. Sci.* (July 2014).

[4] B.E. Logan and K. Rabaey, Conversion of Wastes into Bioelectricity and Chemicals by Using Microbial Electrochemical Techniques, *Science* 337, 686–690 (10 Aug 2012).

[5] H.H. He, M.H. Zhou, J. Yang, Y.H. Hu and Y.Y. Zhao, Simultaneous wastewater treatment, electricity generation and biomass production by an immobilized photosynthetic algal microbial fuel cell, *Bioprocess. Biosyst. Eng.* 37, 873–880 (2014).

[6] M.R. Morgenstern and D.M. Mackie, "Design of a Boost Converter Optimized for High Efficiency with Low-Voltage and Low-Current Hybrid Microbial Fuel Cell Sources," Army Research Laboratory Technical Report ARL-TR-6463, May 2013.

[7] D. Cao and S.H. Bergens, A direct 2-propanol polymer electrolyte fuel cell, *J. Power Sources* 124, 12–17 (2003).

[8] A. Dewan, H. Beyenal, and Z. Lewandowski, Intermittent Energy Harvesting Improves the Performance of Microbial Fuel Cells, *Environ. Sci. Technol.* 43, no. 12, 4600–4605 (2009).

References

1. D.M. Mackie, S. Liu, M. Benyamin, R. Ganguli, and J.J. Sumner, *J. Power Sources* 232 (2013) 34–41.
2. R.C. Saxena, D.K. Adhikari, and H.B. Goyal, *Renewable & Sustainable Energy Reviews* 13 (2009) 167–178.
3. P. Malati, P. Mehrotra, P. Minoofar, D.M. Mackie, J.J. Sumner, and R. Ganguli, submitted *Energy & Fuels*.
4. B.E. Logan and K. Rabaey, *Science* 337 (2012) 686–690.
5. H.H. He, M.H. Zhou, J. Yang, Y.H. Hu and Y.Y. Zhao, *Bioprocess. Biosyst. Eng.* 37 (2014) 873–880.
6. M.R. Morgenstern and D.M. Mackie, Army Research Laboratory Technical Report ARL-TR-6463 (2013).
7. D. Cao and S.H. Bergens, *J. Power Sources* 124 (2003) 12–17.
8. A. Dewan, H. Beyenal, and Z. Lewandowski, *Environ. Sci. Technol.* 43 (2009) 4600–4605.